Photoemission insight into the heavy-fermion behavior in $Ce_{0.85}Yb_{0.15}CoIn_5$

Q. Y. Chen,[1,*] Z. F. Ding,[2] Z. H. Zhu,[2] C. H. P. Wen,[2] Y. B. Huang,[3] P. Dudin,[4] L. Shu,[2] and D. L. Feng[2,5,6]

[1]*Science and Technology on Surface Physics and Chemistry Laboratory, Mianyang 621908, China*

[2]*State Key Laboratory of Surface Physics and Department of Physics, Fudan University, Shanghai 200433, China*

[3]*Shanghai Institute of Applied Physics, Chinese Academy of Sciences, Shanghai 201204, China*

[4]*Diamond Light Source, Harwell Science and Innovation Campus, Didcot OX11 0DE, United Kingdom*

[5]*Hefei National Laboratory for Physical Science at Microscale, CAS Center for Excellence in Quantum Information and Quantum Physics, and Department of Physics, University of Science and Technology of China, Hefei 230026, China*

[6]*Collaborative Innovation Center of Advanced Microstructures, Nanjing 210093, China*

(Received 20 June 2019; revised manuscript received 3 November 2019; published 8 January 2020)

The energy scales in rare-earth-based heavy-fermion compounds are relatively small, which can be easily tuned by applying pressure, magnetic field, or chemical doping. By substituting Yb for Ce on the rare-earth site, the ground state of superconductivity can be smoothly suppressed without the appearance of an apparent quantum critical point, and a number of remarkable phenomena have been observed. The slight changes in the electronic structure are supposed to dominate the underlying physics in these compounds. In the present study, we provide an electronic structure study of $Ce_{0.85}Yb_{0.15}CoIn_5$ with a superconducting state but suppressed transition temperature by angle-resolved photoemission spectroscopy, and the results are compared with $CeCoIn_5$. We find that the f electrons in $Ce_{0.85}Yb_{0.15}CoIn_5$ are itinerant, forming the weakly dispersive hybridized band at low temperature. More interestingly, the hybridization strength between the f electrons and conduction electrons in $Ce_{0.85}Yb_{0.15}CoIn_5$ is comparable with $CeCoIn_5$. Further temperature-dependent measurements provide direct evidence of the localized-to-itinerant crossover behavior of the $4f$ electrons in this compound.

DOI: 10.1103/PhysRevB.101.045105

I. INTRODUCTION

The heavy-fermion compound $CeCoIn_5$ is a prototypical system to study the strong correlations between the f electrons and conduction electrons, which gives rise to a number of remarkable exotic properties, such as the unconventional superconductivity [1], non-Fermi-liquid behavior [2], quantum criticality [3,4], and the potentially exotic pairing states such as the Fulde-Ferrell-Larkin-Ovchinnikov state [5]. $CeCoIn_5$ has a relatively high superconducting transition temperature (T_c) of 2.3 K, and neutron-scattering studies provide direct evidence for an antiferromagnetic quantum critical point (QCP) in $CeCoIn_5$ [6], which can be tuned by pressure, magnetic field, or chemical doping. $CeCoIn_5$ is a good platform to study the substitution effect on the ground-state properties [7], since its stoichiometry is stable and sizable and clean single crystals can be obtained. For example, substituting Rh with Co or Ir tunes the ground state away from the magnetic ordering toward bulk superconductivity [8]. The ground state of $CeCoIn_5$ can be smoothly tuned from a superconducting state to an antiferromagnetic state via Cd and Hg substitution for In [9–13].

Ce(III)($4f^1$) has a single electron in its f shell and Yb(III)($4f^{13}$) has 13 f electrons, only missing one electron to complete the f shell, so Yb is generally considered to be the hole analog of Ce [7]. By substituting Yb for Ce on the rare-earth site, a number of remarkable phenomena have been observed. Although both T_c and the electronic specific heat coefficient are suppressed by Yb doping [7,14], the suppression of T_c is much less than other rare-earth substitutions [15,16]. It is also interesting that the Ce valence remains nearly unchanged from 3+ for all x concentrations, while the Yb valence for $x \leqslant 0.2$ increases rapidly with decreasing x from 2.3+ toward 3+ [7,17]. Investigation of the evolution of the field-induced QCP in $Ce_{1-x}Yb_xCoIn_5$ found that although the field-induced QCP has been suppressed by Yb doping, it has little impact on both the unconventional superconductivity and the non-Fermi-liquid behavior [18].

The topology and size of the Fermi surface is proposed to be a key ingredient for understanding the richness and complexity of the physical properties observed in the heavy-fermion cerium-115 compounds [1,19–23]. In particular, the low-energy electronic structure is expected to be an important issue, which is closely related to the exotic physical properties of the strongly correlated electron systems. Angle-resolved photoemission spectroscopy (ARPES) is a powerful technique which can reveal both the shape and size of the Fermi surface. An earlier ARPES study on $Ce_{1-x}Yb_xCoIn_5$ found that the electronic structure along the $\Gamma - X$ direction is not sensitive to the Yb substitution, suggesting that the Kondo hybridization of Ce f electrons with the conduction electrons is not affected by the presence of Yb impurities in the lattice [7]. Later on, it was revealed by another group that an obvious cross-section area reduction of two Fermi surface sheets was observed between $CeCoIn_5$ and $YbCoIn_5$ by ARPES Fermi surface mappings, and also a proportional size change can be found for $Ce_{0.8}Yb_{0.2}CoIn_5$ [17]. This indicates that the f electrons in $Ce_{0.8}Yb_{0.2}CoIn_5$ take part in the Fermi surface construction, resulting in the size change of the Fermi surface.

*sheqiuyun@126.com

The above-mentioned contrasting results on the f-electron behavior in Yb-doped $CeCoIn_5$ require more detailed and high-resolution ARPES studies. Moreover, the energy scales in these heavy-fermion systems are normally small, which makes it difficult to trace the subtle change of the f electrons by normal ARPES measurements. Fortunately, on-resonant ARPES at the Ce $4d-4f$ transition could largely enhance the f-electron photoemission matrix element, which is proven to be an effective way to explore the f-electron behavior in heavy-fermion compounds [24–26].

Another important issue in heavy-fermion systems is about the localized-to-itinerant crossover behavior of the f electrons. At high temperature, they are local moments, and with decreasing temperature the interplay between the local f moments and the conduction electrons leads to the formation of a "large" Fermi surface with f-electron contribution. This temperature-induced localized-to-itinerant crossover of f electrons has been demonstrated by the dynamical mean-field theory (DMFT) calculations [23,27]. However, despite the many efforts devoted, experimentally there are only a few cases that address this localized-to-itinerant crossover behavior in heavy-fermion compounds [25,26,28,29].

In the present study, we provide a resonant ARPES study of the heavy-fermion compound $Ce_{0.85}Yb_{0.15}CoIn_5$. Detailed studies of the Fermi surface topology and band structure are reported. The main feature of the electronic structure in $Ce_{0.85}Yb_{0.15}CoIn_5$ is dominated by the conducting bands observed in $CeCoIn_5$. We find that the f electrons in $Ce_{0.85}Yb_{0.15}CoIn_5$ take part in the Fermi surface formation, and the hybridization strength is comparable with its parent compound $CeCoIn_5$. No obvious change is observed for the two-dimensional α band with decreasing temperature, while the other two conducting bands hybridize with the f bands to form a "large" Fermi surface. Our results provide direct evidence of the localized-to-itinerant crossover behavior of the f electrons in $Ce_{0.85}Yb_{0.15}CoIn_5$ as a function of temperature.

II. EXPERIMENTAL DETAILS

High-quality single crystals of $Ce_{0.85}Yb_{0.15}CoIn_5$ were synthesized using an indium self-flux method. Details can be found in Ref. [30]. Figures 1 and 2 show the results of work performed at the "Dreamline" beam line of the Shanghai Synchrotron Radiation Facility (SSRF) with a Scienta DA30 analyzer. Both linear-vertical (LV)- and linear-horizontal (LH)-polarized photons were used. The vacuum was better than 5×10^{-11} mbar at 17 K. The energy resolution was 17 meV for 121-eV photons, and the angular resolution was 0.2°. Temperature-dependent ARPES measurements in Figs. 3–5 were performed from a high temperature of 200 K to a low temperature of 9 K at the Beamline I05-ARPES end station of the Diamond Light Source, equipped with a Scienta R4000 analyzer. The samples were cleaved along the c axis before ARPES measurements at 200 K. The typical angular resolution was 0.2° and the overall energy resolution was better than 15 meV. The vacuum was kept below 9×10^{-11} mbar.

III. RESULTS AND DISCUSSIONS

The experimental setup for our ARPES measurements is shown in Fig. 1(a). Figure 1(b) displays the photoemission intensity map of $Ce_{0.85}Yb_{0.15}CoIn_5$ at 12 K taken with 121-eV LH-polarized photons. The Fermi surface is similar to that of

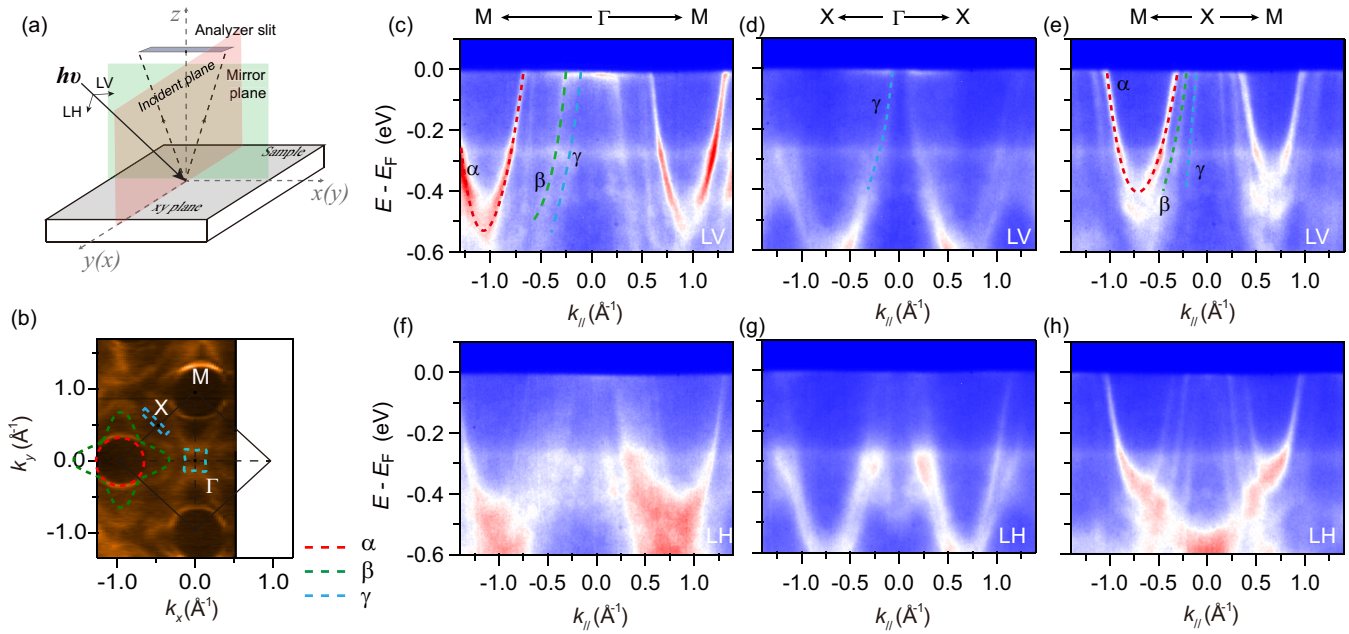

FIG. 1. Fermi surface and band structure of $Ce_{0.85}Yb_{0.15}CoIn_5$ taken with 121-eV photons at 15 K. (a) Experimental setup for our ARPES measurements. Here linear vertical (LV) polarization represents the direction of the photons which is perpendicular to the mirror plane in (a), while linear horizontal (LH) denotes the direction parallel to the mirror plane [31]. (b) Photoemission intensity map of $Ce_{0.85}Yb_{0.15}CoIn_5$ integrated over a window of $(E_F-20\,\text{meV}, E_F+20\,\text{meV})$. Fermi surface contours are drawn with respective colors in the dashed lines. The square highlighted corresponds to the first Brillouin zone. (c–e) Photoemission intensity distribution plots along (c) ΓM, (d) ΓX, and (e) MX with LV-polarized light. (f–h) Photoemission intensity distribution plots along (c) ΓM, (d) ΓX, and (e) MX with LH-polarized light.

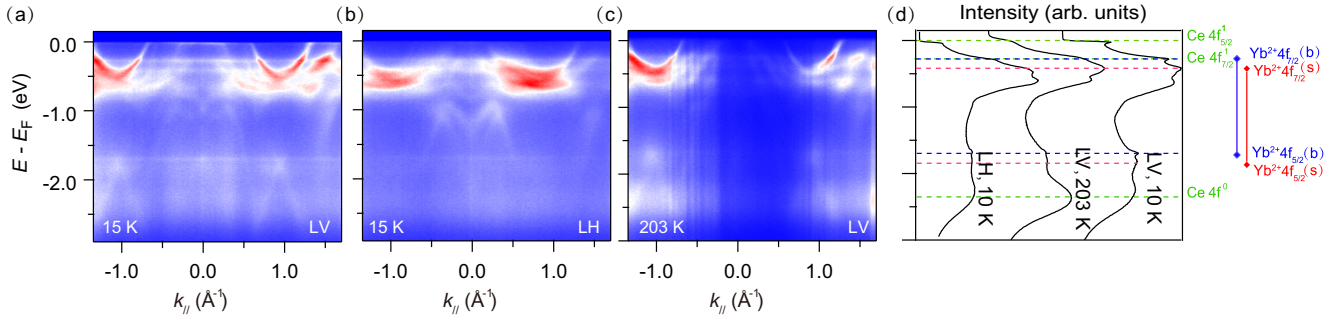

FIG. 2. Photoemission intensity distributions of $Ce_{0.85}Yb_{0.15}CoIn_5$ along ΓM taken at 15 K with (a) 121-eV LV-polarized photons and (b) LH-polarized photons. (c) Photoemission intensity distributions of $Ce_{0.85}Yb_{0.15}CoIn_5$ along $\Gamma - M$ taken at 203 K with LV-polarized photons. (d) Angle-integrated energy distribution curves (EDCs) of $Ce_{0.85}Yb_{0.15}CoIn_5$ taken with different polarized photons and temperature; the f-band positions for Ce and Yb are highlighted [7,17,32,33]. The spectra have been normalized by the intensity height at 2.8 eV binding energy.

$CeCoIn_5$ [26] with one small holelike square Fermi pocket around the Brillouin zone center and two electronlike Fermi pockets around the zone corner. One is a flower-shaped β pocket and the other one is a rounded α pocket. Also, a narrow racetrack pocket can be observed extending to the middle of the zone boundary around the X point, which is also from the γ band. Figures 1(c)–1(e) present the detailed band dispersions along several high-symmetry directions. Along the ΓM direction, three bands can be observed crossing the Fermi level, which can be assigned to the α, β, and γ bands, respectively. The α band is paraboliclike, and the holelike γ band encloses the Γ point forming the squarelike Fermi pocket around the Brillouin zone center. The dispersions of the α, β, and γ bands can be more clearly observed from the band structure along the MX direction. Because the slit of the analyzer for our ARPES measurements is vertical to the ground, the LV polarization can be used to detect the even-parity orbitals and z components, while the LH polarization can be used to detect the odd-parity orbitals. From the comparison of the band structure taken with LV and LH polarizations, we found that for the α, β, and γ bands, although there is an intensity difference, they can be detected by both LH and LV polarizations, indicating they are not pure orbitals.

Figure 2 presents the photoemission intensity plots of $Ce_{0.85}Yb_{0.15}CoIn_5$ using 121-eV photons at the Ce $4d - 4f$ transition to enhance the Ce $4f$ cross section. From Fig. 2(a), several flat bands can be observed, located at 0.026, 0.278, 0.418, 1.696, 1.830, and 2.267 eV binding energy (BE), respectively. Among them, the weakly dispersive flat band at 2.267 eV corresponds to the $4f^0$ final state associated with the cost of removing one electron from the trivalent Ce ion ($4f^1 \longrightarrow 4f^0$), compared with that of 2.2 eV in $CeCoIn_5$. The other two flat bands located at 0.026 and 0.278 eV BE can be attributed to the tail of the Kondo resonance and its spin-orbit-split component [32]. Previous study on the Yb valence change in $Ce_{1-x}Yb_xCoIn_5$ has shown that the Yb valence for $x \leqslant 0.2$ increases rapidly with decreasing x from 2.3 toward 3+ [17], which indicates that $Ce_{0.85}Yb_{0.15}CoIn_5$

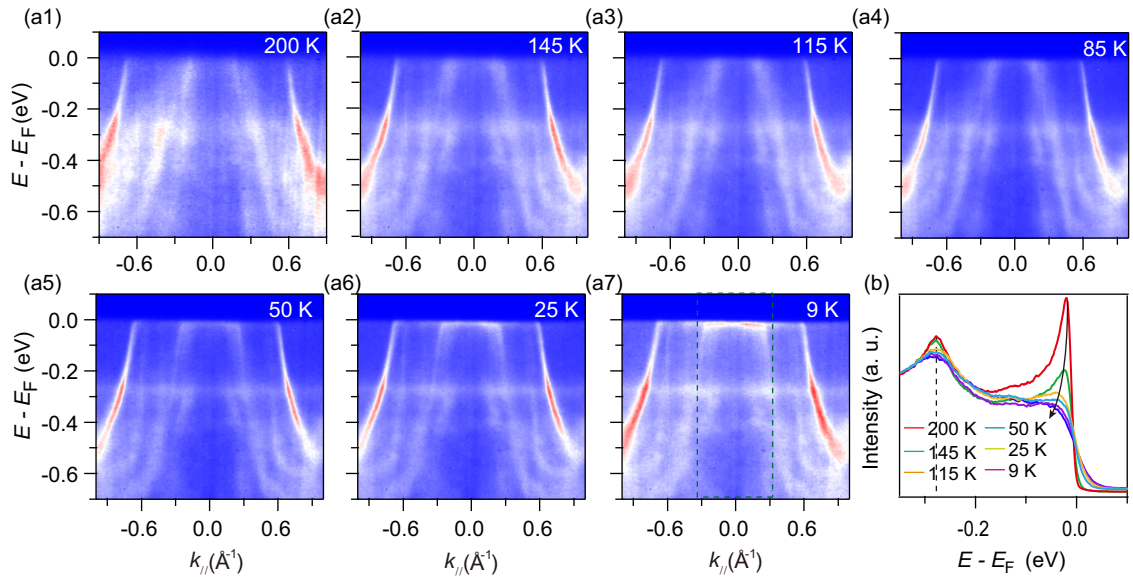

FIG. 3. (a1–a7) Temperature dependence of the photoemission intensity plots of $Ce_{0.85}Yb_{0.15}CoIn_5$ along ΓM taken with 121-eV LV-polarized photons. (b) Temperature dependence of the EDCs around the Γ point. The integrated window is marked with the green dashed block.

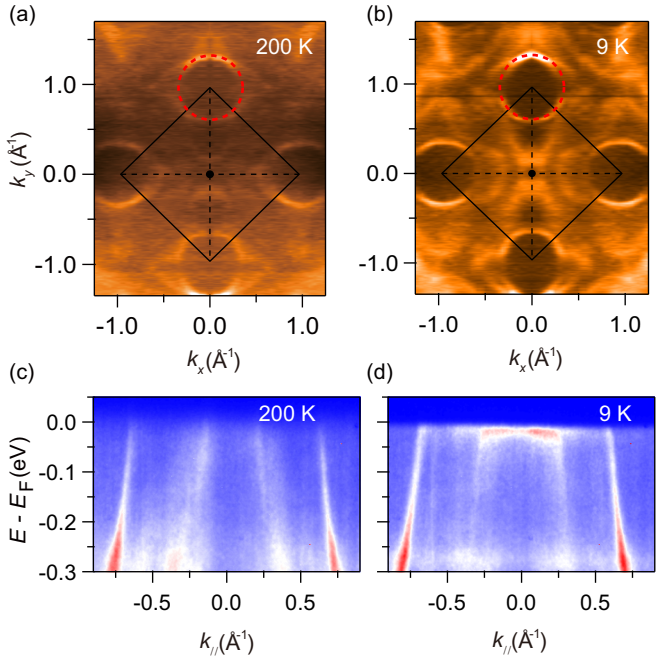

FIG. 4. (a), (b) Photoemission intensity map of $Ce_{0.85}Yb_{0.15}CoIn_5$ taken with 121-eV LV-polarized photons along ΓM at (a) 200 K and (b) 9 K. (c, d) Photoemission intensity plots of $Ce_{0.85}Yb_{0.15}CoIn_5$ along ΓM taken with 121-eV LV-polarized photons at (c) 200 K and (d) 9 K.

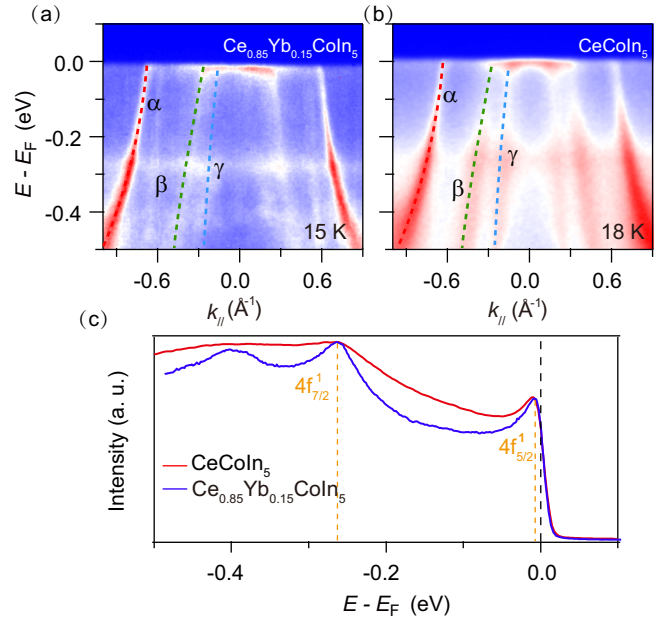

FIG. 5. (a) Photoemission intensity plot of $Ce_{0.85}Yb_{0.15}CoIn_5$ taken with 121-eV LV-polarized photons along ΓM at 15 K. (b) Photoemission intensity plot of $CeCoIn_5$ along ΓM taken with 121-eV LV-polarized photons at 18 K, which has been reported in our previous study [26]. We plot it here to give a direct impression of the band-structure change in the two compounds. (c) Comparison of the angle-integrated EDCs between $Ce_{0.85}Yb_{0.15}CoIn_5$ and $CeCoIn_5$, which is normalized by the intensity of the $4f^1_{7/2}$ state.

is in the mixed-valence region. In an intermediate-valence Yb compound, the Yb^{3+} multiplet ($4f^{13} \rightarrow 4f^{12}$) normally locates at the binding energy between 5.5 and 8.5 eV, and the Yb^{2+} doublet at the lower binding energy of 0–2.5 eV ($4f^{14} \rightarrow 4f^{13}$). Following previous studies [7,17,33], we can identify different f states for Yb in Fig. 2(d). The blue one is the final-state $F_{5/2}$-$F_{7/2}$ doublet of the Yb^{2+} photoemission process $4f^{14} \rightarrow 4f^{13}$ from deep-lying Yb layers. Two peaks at higher binding energy marked red with the same energy separation as the $F_{5/2}$-$F_{7/2}$ doublet are due to Yb^{2+} from the surface. Such surface-shifted Yb^{2+} peaks are well known [17,33]. It is noteworthy that one of the Yb^{2+} states has a similar energy level with Ce $4f^1_{7/2}$, which makes it difficult to separate them from each other.

By comparing the ARPES data taken at different polarization conditions, it is interesting to note that the $4f^1_{5/2}$ component is quite sensitive to the polarization of the light, which can be strongly enhanced with LV polarization, indicating the mainly even-parity character of the f orbitals. This different behavior with polarization is also consistent with that observed in $CeCoIn_5$ [26]. Figure 2(c) shows the ARPES data taken at 203 K for $Ce_{0.85}Yb_{0.15}CoIn_5$. By comparing the EDCs taken at 203 and 15 K, we find that the position of the $4f^0$ state shifts to higher BE at 203 K, and, more importantly, the intensity of the $4f^1_{7/2}$ state gets broadened at high temperature. The absence of the $4f^1_{5/2}$ peak near the Fermi level (E_F) can be considered an indication of an almost localized f-electron character. This behavior of the f states is in analogy to what we observed in the ordered Ce films during the α-γ phase transition [34].

In Fig. 2, we observed an obvious change of the f states in $Ce_{0.85}Yb_{0.15}CoIn_5$ between 203 and 15 K. To investigate the detailed evolution of the f states as a function of temperature in $Ce_{0.85}Yb_{0.15}CoIn_5$, we performed temperature-dependent resonant ARPES measurements. Figures 3(a1)–3(a7) show the evolution of the band structure with temperature taken with 121-eV LV-polarized photons. Here 121-eV photons (the energy of the Ce $4d - 4f$ transition) are used to realize a resonant enhancement of the Ce $4f$ photoionization cross section. At a high temperature of 200 K, the electronic structure is dominated by the above-mentioned three conduction bands of α, β, and γ. With lowering temperature, the spectral weight near E_F, especially around the Γ point, gradually increases and forms a weakly dispersive band at low temperature. This temperature-dependent behavior can also be traced from the EDCs around the Γ point in Fig. 3(b). From Fig. 3(b), the position of the $4f^1_{5/2}$ state shifts to higher BE, while the position of its spin-orbit-split component $4f^1_{7/2}$ almost remains the same. From Fig. 3(a4), the weakly dispersive f band already becomes discernible at around 85 K, which is much higher than the coherence temperature of 50 K and is consistent with that observed in $CeCoIn_5$ [26].

Figures 4(a) and 4(b) show the comparison of the photoemission intensity maps for $Ce_{0.85}Yb_{0.15}CoIn_5$ taken at 200 and 9 K, and zoomed-in ARPES data of the band structure are displayed in Figs. 4(c) and 4(d). At 200 K, the conduction bands all show linear dispersion, and weakly dispersive f bands can be observed near the Fermi level at 9 K. While

no obvious difference is observed for the conducting α band, significant enhancement can be observed around the Γ point for both the β and γ bands. From Figs. 4(a) and 4(b), it is easy to trace the size change of the α pocket, and we find that the size for the α pocket is almost the same at high and low temperature, indicating nearly absent hybridization between the f band and the α band. Meanwhile, an obvious difference is observed for the β and γ bands, which further demonstrates that the f bands in $Ce_{0.85}Yb_{0.15}CoIn_5$ mainly hybridize with the β and γ bands. However, due to the overlap between the β and γ bands, especially after hybridization with the f bands at low temperature, it is hard to give an accurate estimation of the size change of these two bands.

In Fig. 5, we further present a comparison of the electronic structure between $Ce_{0.85}Yb_{0.15}CoIn_5$ and its parent compound $CeCoIn_5$. In $CeCoIn_5$, three conduction bands named α, β, and γ can be found in Fig. 5(b). For $Ce_{0.85}Yb_{0.15}CoIn_5$, the spectrum is also dominated by these three bands, and the dispersion of the three bands is similar to that of $CeCoIn_5$. Weakly dispersive f bands can be found in the two compounds near the Fermi level, which is due to the hybridization between the f bands and conduction bands, indicating that the f electrons participate in the construction of the Fermi surface, forming a "large" Fermi surface. Figure 5(c) shows the comparison of the EDCs in the two compounds, and the positions of both the $4f^1_{5/2}$ and $4f^1_{7/2}$ states remain the same. More importantly, if we normalize the spectra by the intensity height of the $4f^1_{7/2}$ state, the intensity of the $4f^1_{5/2}$ state in the two compounds remains almost the same. This provides evidence that the hybridization strength between the f bands and the conduction bands is comparable in the two compounds. This is consistent with the de Haas–van Alphen (dHvA) results that changes of the Fermi surface topology can be observed until $x = 0.2$ and drastic reconstruction of the Fermi surface can be observed above $x = 0.55$ [35]. In heavy-fermion systems, at low temperature the interplay between the local f moments with the itinerant conduction electrons leads to the formation of heavy-quasiparticle bands and a huge density of states near the Fermi energy. At this stage, both the f electrons and conduction electrons participate in the construction of the Fermi surface, resulting in a so-called large Fermi surface. Upon weakening of the interaction between the f electrons and conduction electrons, like increasing temperature, the f electrons can be recognized as local moments, which do not take part in the Fermi surface formation, leading to a "small" Fermi surface without f-electron contribution. This temperature-induced localized-to-itinerant transition of the f electrons has been proven by DMFT calculations [23,27]. However, experimentally there are only a few cases that can provide evidence for this localized-to-itinerant transition [25,26,28,29].

In the present study of $Ce_{0.85}Yb_{0.15}CoIn_5$, we found that the f electrons are mainly localized at 200 K. Upon lowering temperature, the f spectral weight gradually develops near the Fermi level close to the Γ point, and finally forms the weakly dispersive hybridized band at low temperature. This provides direct evidence of the localized-to-itinerant crossover behavior of the f electrons in this system. However, we also found that different conduction bands show various behavior. The α band hardly hybridizes with the f band even at the lowest measuring temperature, and the size of the α pocket almost remains the same. However, both the β and γ bands hybridize with the f bands at low temperature, forming the weakly dispersive hybridized bands. This band-dependent c-f hybridization behavior is in line with the band-dependent hybridization behavior of the f electrons observed in $CeRhIn_5$ [36] and makes it more difficult to connect the onset temperature of the appearance of the f spectral weight with the coherence temperature observed from the resistivity data. Transport measurements are normally collective effects, while ARPES measurements have k-space resolution. Especially considering the significantly different behavior between different bands, these different temperature scales should not be lumped together.

Previous dHvA investigations of the Fermi-surface evolution with Yb substitution in $Ce_{1-x}Yb_xCoIn_5$ found that for a small Yb concentration of $x = 0.1$, both the band structure and effective mass remain nearly unchanged compared to its parent compound $CeCoIn_5$. Changes of the Fermi surface topology can be observed at $x = 0.2$, leading to a drastic reconstruction above $x = 0.55$ [35]. Later on, a combined study of photoemission x-ray absorption found that the Ce valence remains nearly unchanged from 3+ for all x concentrations, while the Yb valence for $x \leqslant 0.2$ increases rapidly with decreasing x from 2.3+ toward 3+ [17]. In the present study, we find that the hybridization strength between the f electrons and conduction electrons in $Ce_{0.85}Yb_{0.15}CoIn_5$ is comparable with that of its parent compound $CeCoIn_5$, and the Fermi surface retains a "large" Fermi surface with f-electron contribution. This is consistent with the nearly unchanged Fermi-surface topology and effective mass by dHvA measurements for the x concentration below $x = 0.2$.

Two different scenarios have been proposed to explain the role of Yb in $Ce_{1-x}Yb_xCoIn_5$. Dudy *et al.* [17] proposed from extended x-ray absorption fine structure (EXAFS) and ARPES measurements that there are two interlaced but independent networks in $Ce_{1-x}Yb_xCoIn_5$ that couple to the conduction band: one network of Ce ions in the heavy-fermion limit, and one network of Yb ions in the strongly intermediate-valence limit. While Yb substitutes into the $CeCoIn_5$ lattice, the $CeCoIn_5$ network appears to act independently of the regions of $YbCoIn_5$, and the heavy-fermion state preserves its coherence up to rather large doping levels. They also find that the electronic structure along $\Gamma - X$ is not sensitive to the Yb substitution, suggesting that the Kondo hybridization between the Ce f electrons and the conduction electrons is not affected by the presence of Yb impurities in the lattice. They also found that the Yb valence for $x \leqslant 0.2$ increasing rapidly with decreasing x from 2.3 toward 3+, and their ARPES results also observed Fermi-surface size reduction of two sheets from $CeCoIn_5$ to $YbCoIn_5$ [17]. Shu *et al.* suggested a correlated electron state having cooperative valence fluctuations of Yb and Ce [14]. dHvA results by Polyakov *et al.* found that changes of the Fermi surface topology can be observed at $x = 0.2$, and a drastic reconstruction of the Fermi surface occurs above $x = 0.55$ [35]. From our results, a difference can be found for the electronic structure at much higher binding energy; however, the low-energy electronic structure of $Ce_{1-x}Yb_xCoIn_5$ is similar to that of $CeCoIn_5$, and this suggests that Yb can be considered as forming disordered

impurities in $CeCoIn_5$. It is also noteworthy that the Yb state is far away from the Fermi level, and it does not contribute to the low-energy physics of $Ce_{0.85}Yb_{0.15}CoIn_5$. This is consistent with its higher Kondo temperature [7].

IV. CONCLUSION

In summary, we present an electronic structure study of $Ce_{0.85}Yb_{0.15}CoIn_5$ with a superconducting ground state. The main feature of the electronic structure of $Ce_{0.85}Yb_{0.15}CoIn_5$ is dominated by the observed conduction bands in $CeCoIn_5$. We observe a nearly flat band near the Fermi level around the Γ point, which is gradually suppressed with increasing temperature. On-resonant temperature-dependent measurements provide direct evidence for the localized-to-itinerant crossover behavior of the f electrons in $Ce_{0.85}Yb_{0.15}CoIn_5$. More importantly, we found that the hybridization strength between the f electrons and conduction electrons is comparable in $Ce_{0.85}Yb_{0.15}CoIn_5$ and $CeCoIn_5$. Our results may be important for understanding the f-electron behavior in different heavy-fermion systems, and should provide an important clue for establishing the relationship between the ground-state properties and the hybridization strength between the f electrons and conduction electrons. Further research will be concentrated on the evolution of the electronic structure as a function of the Yb doping level.

ACKNOWLEDGMENTS

This work is supported by the National Natural Science Foundation of China (Grants No. 11874330, No. U1630248, No. 11504341, and No. 11504342), the Science Challenge Project (Grant No. TZ2016004), and the National Key Research and Development Program of China (Grant No. 2017YFA0303104). We also want to thank Diamond Light Source for time on Beamline I05 under Proposal No. SI1914 and beam time at the Dream-line beam line of the Shanghai Synchrotron Radiation Facility (SSRF).

[1] C. Petrovic, P. G. Pagliuso, M. F. Hundley, R. Movshovich, J. L. Sarrao, J. D. Thompson, Z. Fisk, and P. Monthoux, Heavy-fermion superconductivity in $CeCoIn_5$ at 2.3 K, J. Phys.: Condens. Matter **13**, L337 (2001).

[2] J. S. Kim, J. Alwood, G. R. Stewart, J. L. Sarrao, and J. D. Thompson, Specific heat in high magnetic fields and non-Fermi-liquid behavior in $CeMIn_5$(M = Ir, Co), Phys. Rev. B **64**, 134524 (2001).

[3] V. A. Sidorov, M. Nicklas, P. G. Pagliuso, J. L. Sarrao, Y. Bang, A. V. Balatsky, and J. D. Thompson, Superconductivity and Quantum Criticality in $CeCoIn_5$, Phys. Rev. Lett. **89**, 157004 (2002).

[4] S. Singh, C. Capan, M. Nicklas, M. Rams, A. Gladun, H. Lee, J. F. DiTusa, Z. Fisk, and S. Wirth, Probing the Quantum Critical behavior of $CeCoIn_5$ visa Hall Effect Measurements, Phys. Rev. Lett. **98**, 057001 (2007).

[5] C. F. Miclea, M. Nicklas, D. Parker, K. Maki, J. L. Sarrao, J. D. Thompson, G. Sparn, and F. Steglich, Pressure Dependence of the Fulde-Ferrell-Larkin-Ovchinnikov State in $CeCoIn_5$, Phys. Rev. Lett. **96**, 117001 (2006).

[6] C. Stock, C. Broholm, J. Hudis, H. J. Kang, and C. Petrovic, Spin Resonance in the d-Wave Superconductor $CeCoIn_5$, Phys. Rev. Lett. **100**, 087001 (2008).

[7] C. H. Booth, T. Durakiewicz, C. Capan, D. Hurt, A. D. Bianchi, J. J. Joyce, and Z. Fisk, Electronic structure and f-orbital occupancy in Yb-substituted $CeCoIn_5$, Phys. Rev. B **83**, 235117 (2011).

[8] V. S. Zapf, E. J. Freeman, E. D. Bauer, J. Petricka, C. Sirvent, N. A. Frederick, R. P. Dickey, and M. B. Maple, Coexistence of superconductivity and antiferromagnetism in $CeRh_{1-x}Co_xIn_5$, Phys. Rev. B **65**, 014506 (2001).

[9] Y. Tokiwa, R. Movshovich, F. Ronning, E. D. Bauer, P. Papin, A. D. Bianchi, J. F. Raurscher, S. M. Kauzlarich, and Z. Fisk, Anisotropic effect of Cd and Hg doping on the Pauli limited superconductor $CeCoIn_5$, Phys. Rev. Lett. **101**, 037001 (2008).

[10] L. D. Pham, T. Park, S. Maquilong, J. D. Thompson, and Z. Fisk, Reversible Tuning of the Heavy-Fermion Ground State in $CeCoIn_5$, Phys. Rev. Lett. **97**, 056404 (2006).

[11] Y. Chen, W. B. Jiang, C. Y. Guo, F. Ronning, E. D. Bauer, Tuson Park, H. Q. Yuan, Z. Fisk, J. D. Thompson, and Xin Lu, Reemergent Superconductivity and Avoided Quantum Criticality in Cd-Doped $CeIrIn_5$ Under Pressure, Phys. Rev. Lett. **114**, 146403 (2015).

[12] R. G. Goodrich, C. Capan, A. D. Bianchi, Z. Fisk, J. F. DiTusa, I. Vekhter, D. P. Young, L. Balicas, Y.-J. Yo, T. Murphy, J. Y. Cho, and J. Y. Chan, SC-AFM transition in $CeCo(In_{1-x}Cd_x)_5$: de Haas–van Alphen measurements, J. Phys.: Conf. Ser. **273**, 012113 (2011).

[13] M. Nicklas, O. Stockert, T. Park, K. Habicht, K. Kiefer, L. D. Pham, J. D. Thompson, Z. Fisk, and F. Steglich, Magnetic structure of Cd-doped $CeCoIn_5$, Phys. Rev. B **76**, 052401 (2007).

[14] L. Shu, R. E. Baumbach, M. Janoschek, E. Gonzales, K. Huang, T. A. Sayles, J. Paglione, J. O'Brien, J. J. Hamlin, D. A. Zocco, P.-C. Ho, C. A. McElroy, and M. B. Maple, Correlated Electron State in $Ce_{1-x}Yb_xCoIn_5$ Stabilized by Cooperative Valence Fluctuations, Phys. Rev. Lett. **106**, 156403 (2011).

[15] C. Petrovic, S. L. Bud'ko, V. G. Kogan, and P. C. Canfield, Effects of La substitution on the superconducting state of $CeCoIn_5$, Phys. Rev. B **66**, 054534 (2002).

[16] R. Hu, Y. Lee, J. Hudis, V. F. Mitrovic, and C. Petrovic, Composition and field-tuned magnetism and superconductivity in $Nd_{1-x}Ce_xIn_5$, Phys. Rev. B **77**, 165129 (2008).

[17] L. Dudy, J. D. Denlinger, L. Shu, M. Janoschek, J. W. Allen, and M. B. Maple, Yb valence change in $Ce_{1-x}Yb_xCoIn_5$ from spectroscopy and bulk properties, Phys. Rev. B **88**, 165118 (2013).

[18] T. Hu, Y. P. Singh, L. Shu, M. Janoschek, M. Dzero, M. B. Maple, and C. C. Almasan, Non-Fermi liquid regimes with and without quantum criticality in $Ce_{1-x}Yb_xCoIn_5$. Proc. Natl. Acad. Sci. USA **110**, 7160 (2013).

[19] M. P. Allan, F. Massee, D. K. Morr, J. Van Dyke, A. W. Rost, A. P. Mackenzie, C. Petrovic, and J. C. Davis, Imaging Cooper pairing of heavy fermions in $CeCoIn_5$, Nat. Phys. **9**, 468 (2013).

[20] B. B. Zhou, S. Misra, E. H. da Silva Neto, P. Aynajian, R. E. Baumbach, J. D. Thompson, E. D. Bauer, and A. Yazdani,

Visualizing nodal heavy fermion superconductivity in $CeCoIn_5$, Nat. Phys. **9**, 474 (2013).

[21] E. J. Singley, D. N. Basov, E. D. Bauer, and M. B. Maple, Optical conductivity of the heavy fermion superconductor $CeCoIn_5$, Phys. Rev. B **65**, 161101(R) (2002).

[22] K. Haule, C.-H. Yee, and K. Kim, Dynamical mean-field theory within the full-potential methods: Electronic structure of $CeIrIn_5$, $CeCoIn_5$, and $CeRhIn_5$, Phys. Rev. B **81**, 195107 (2010).

[23] H. C. Choi, B. I. Min, J. H. Shim, K. Haule, and G. Kotliar, Temperature-Dependent Fermi Surface Evolution in Heavy Fermion $CeIrIn_5$, Phys. Rev. Lett. **108**, 016402 (2012).

[24] Y. Zhang, W. Feng, X. Lou, T. L. Yu, X. G. Zhu, S. Y. Tan, B. K. Yuan, Y. Liu, H. Y. Lu, D. H. Xie, Q. Liu, W. Zhang, X. B. Luo, Y. B. Huang, L. Z. Luo, Z. J. Zhang, X. C. Lai, and Q. Y. Chen, Direct observation of heavy quasiparticles in the Kondo-lattice compound $CeIn_3$, Phys. Rev. B **97**, 045128 (2018).

[25] S. Jang, J. D. Denlinger, J. W. Allen, V. S. Zapf, M. B. Maple, J. N. Kim, B. G. Jang, and J. H. Shim, Evolution of the Kondo lattice electronic structure above the transport coherence temperature, arXiv:1704.08247.

[26] Q. Y. Chen, D. F. Xu, X. H. Niu, J. Jiang, R. Peng, H. C. Xu, C. H. P. Wen, Z. F. Ding, K. Huang, L. Shu, Y. J. Zhang, H. Lee, V. N. Strocov, M. Shi, F. Bisti, T. Schmitt, Y. B. Huang, P. Dudin, X. C. Lai, S. Kirchner, H. Q. Yuan, and D. L. Feng, Direct observation of how the heavy-fermion state develops in $CeCoIn_5$, Phys. Rev. B **96**, 045107 (2017).

[27] J. H. Shim, K. Haule, and G. Kotliar, Modeling the localized-to-itinerant electronic transition in the heavy fermion system $CeIrIn_5$, Science **318**, 1615 (2007).

[28] S.-K. Mo, W. S. Lee, F. Schmitt, Y. L. Chen, D. H. Lu, C. Capan, D. J. Kim, Z. Fisk, C.-Q. Zhang, Z. Hussain, and Z.-X. Shen, Emerging coherence with unified energy, temperature, and lifetime scale in heavy fermion $YbRh_2Si_2$, Phys. Rev. B **85**, 241103(R) (2012).

[29] S.-I. Fujimori, Y. Saitoh, T. Okane, A. Fujimori, H. Yamagami, Y. Haga, E. Yamamoto, and Y. Onuki, Itinerant to localized transition of f electrons in the antiferromagnetic superconductor UPd_2Al_3, Nat. Phys. **3**, 618 (2007).

[30] Z. F. Ding, J. Zhang, C. Tan, K. Huang, Q. Y. Chen, I. Lum, O. O. Bernal, P.-C. Ho, D. E. MacLaughlin, M. B. Maple, and L. Shu, Renormalizations in unconventional superconducting states of $Ce_{1-x}Yb_xCoIn_5$, Phys. Rev. B **99**, 035136 (2019).

[31] Q. Yao, D. Kaczorowski, P. Swatek, D. Gnida, C. H. P. Wen, X. H. Niu, R. Peng, H. C. Xu, P. Dudin, S. Kirchner, Q. Y. Chen, D. W. Shen, and D. L. Feng, Electronic structure and $4f$-electron character in Ce_2PdIn_8 studied by angle-resolved photoemission spectroscopy, Phys. Rev. B **99**, 081107(R) (2019).

[32] S. Patil, A. Generalov, M. Güttler, P. Kushwaha, A. Chikina, K. Kummer, T. C. Rödel, A. F. Santander-Syro, N. Caroca-Canales, C. Geibel, S. Danzenbächer, Y. Kucherenko, C. Laubschat, J. W. Allen, and D. V. Vyalikh, ARPES view on surface and bulk hybridization phenomena in the antiferromagnetic Kondo lattice $CeRh_2Si_2$, Nat. Commun. **7**, 11029 (2016).

[33] K. Kummer, Yu. Kucherenko, S. Danzenbacher, C. Krellner, C. Geibel, M. G. Holder, L. V. Bekenov, T. Muro, Y. Kato, T. Kinoshita, S. Huotari, L. Simonelli, S. L. Molodtsov, C. Laubschat, and D. V. Vyalikh, Intermediate valence in Yb compounds probed by $4f$ photoemission and resonant inelastic x-ray scattering, Phys. Rev. B **84**, 245114 (2011).

[34] Q. Y. Chen, W. Feng, D. H. Xie, X. C. Lai, X. G. Zhu, and L. Huang, Localized to itinerant transition of f electrons in ordered Ce films on W(110), Phys. Rev. B **97**, 155155 (2018).

[35] A. Polyakov, O. Ignatchik, B. Bergk, K. Götze, A. D. Bianchi, S. Blackburn, B. Prévost, G. Seyfarth, M. Côté, D. Hurt, C. Capan, Z. Fisk, R. G. Goodrich, I. Sheikin, M. Richter, and J. Wosnitza, Fermi surface evolution in Yb-substituted $CeCoIn_5$, Phys. Rev. B **85**, 245119 (2012).

[36] Q. Y. Chen, D. F. Xu, X. H. Niu, R. Peng, H. C. Xu, C. H. P. Wen, X. Liu, L. Shu, S. Y. Tan, X. C. Lai, Y. J. Zhang, H. Lee, V. N. Strocov, F. Bisti, P. Dudin, J.-X. Zhu, H. Q. Yuan, S. Kirchner, and D. L. Feng, Band Dependent Interlayer f-Electron Hybridization in $CeRhIn_5$, Phys. Rev. Lett. **120**, 066403 (2018).